MCB
Journals.ASM.org

# A Novel 4EHP-GIGYF2 Translational Repressor Complex Is Essential for Mammalian Development

**Masahiro Morita,[a] Lian Wee Ler,[a] Marc R. Fabian,[a] Nadeem Siddiqui,[a] Michael Mullin,[b] Valerie C. Henderson,[a] Tommy Alain,[a] Bruno D. Fonseca,[a] Galina Karashchuk,[c] Christopher F. Bennett,[a] Tomohiro Kabuta,[d] Shinji Higashi,[e] Ola Larsson,[f] Ivan Topisirovic,[g,h] Robert J. Smith,[i] Anne-Claude Gingras,[b,j] and Nahum Sonenberg[a]**

Department of Biochemistry and Goodman Cancer Research Centre, McGill University, Montréal, Quebec, Canada[a]; Samuel Lunenfeld Research Institute, Mount Sinai Hospital, Toronto, Ontario, Canada[b]; Department of Ecology and Evolutionary Biology, Brown University, Providence, Rhode Island, USA[c]; Department of Degenerative Neurological Diseases, National Institute of Neuroscience, National Center of Neurology and Psychiatry, Kodaira-shi, Tokyo, Japan[d]; Dementis Research Project, Tokyo Metropolitan Institute of Medical Science, Setagaya-ku, Tokyo, Japan[e]; Department of Oncology-Pathology, Karolinska Institute, Stockholm, Sweden[f]; Lady Davis Institute for Medical Research, SMBD-Jewish General Hospital, McGill University, Montréal, Quebec, Canada[g]; Department of Oncology, McGill University, Montréal, Quebec, Canada[h]; Department of Veterans Affairs Medical Center, Alpert Medical School of Brown University, Providence, Rhode Island, USA[i]; and Department of Molecular Genetics, University of Toronto, Toronto, Ontario, Canada[j]

**The binding of the eukaryotic initiation factor 4E (eIF4E) to the mRNA 5′ cap structure is a rate-limiting step in mRNA translation initiation. eIF4E promotes ribosome recruitment to the mRNA. In *Drosophila*, the eIF4E homologous protein (d4EHP) forms a complex with binding partners to suppress the translation of distinct mRNAs by competing with eIF4E for binding the 5′ cap structure. This repression mechanism is essential for the asymmetric distribution of proteins and normal embryonic development in *Drosophila*. In contrast, the physiological role of the mammalian 4EHP (m4EHP) was not known. In this study, we have identified the Grb10-interacting GYF protein 2 (GIGYF2) and the zinc finger protein 598 (ZNF598) as components of the m4EHP complex. GIGYF2 directly interacts with m4EHP, and this interaction is required for stabilization of both proteins. Disruption of the m4EHP-GIGYF2 complex leads to increased translation and perinatal lethality in mice. We propose a model by which the m4EHP-GIGYF2 complex represses translation of a subset of mRNAs during embryonic development, as was previously reported for d4EHP.**

Translation initiation refers to a series of reactions that culminate in the recruitment of the 80S ribosome to the mRNA (13). This process begins with the recognition of the $m^7$GpppN structure (5′ cap), which is present at the 5′ end of all nuclear transcribed mRNAs, by the eukaryotic translation initiation factor 4F (eIF4F) (39). eIF4E is the 5′ cap-binding subunit of the heterotrimeric eIF4F complex (39). eIF4F also contains the scaffolding protein eIF4G and the RNA helicase eIF4A, which is thought to unwind the secondary structure of the mRNA 5′ untranslated region (5′ UTR) (39). Multiple mechanisms control translation initiation in eukaryotes, many of which impact eIF4E (20). One of the best-studied mechanisms of translation inhibition involves a family of eIF4E-binding proteins (4E-BPs), which interfere with the interaction between eIF4E and eIF4G by competing for a shared binding surface on eIF4E (12, 17, 31). Similarly, the eIF4E transporter (4E-T) also interacts with eIF4E through the same binding site to control translation and the subcellular localization of eIF4E (7, 10). Another mechanism of translational control involves eIF4E-binding proteins that interact with factors bound to a specific subset of mRNAs (32). Proteins such as Cup in *Drosophila* or Maskin in *Xenopus* simultaneously bind the cap-bound eIF4E and sequence-specific RNA-binding proteins, which in turn interact with the 3′ UTR of mRNA (2, 29, 40). These proteins interdict the interaction of eIF4F with the mRNA cap structure and consequently repress translation.

There are three eIF4E family members in mammals, termed eIF4E-1 (eIF4E; gene name, *EIF4E*), eIF4E-2 (or mammalian eIF4E homologous protein [m4EHP]; gene name, *EIF4E2*), and eIF4E-3 (gene name, *EIF4E3*) (21, 33). eIF4E is the major form and has been intensively investigated. In contrast, very little is known regarding the function of eIF4E-3, since its expression has only been detected at the transcript level (21). m4EHP is a widely expressed protein that is 5 to 10 times less abundant than eIF4E (21, 33). m4EHP binds the 5′ cap structure, albeit with ~100- to 200-fold lower affinity than eIF4E (34, 47). In sharp contrast to eIF4E, m4EHP does not bind eIF4G and is therefore unlikely to stimulate translation initiation (21, 33). Instead, m4EHP was predicted to compete with eIF4E for the 5′ cap structure to act as a translation repressor (33). Indeed, such a mechanism involving 4EHP was documented in *Drosophila*, where the morphogen Bicoid binds directly to *Drosophila* 4EHP (d4EHP) and tethers it to the 3′ UTR of *caudal* mRNA to repress its translation (5). Similarly, d4EHP also impairs the translation of *hunchback* mRNA through simultaneous interaction with the 5′ cap and an RNA-binding protein complex (consisting of Nanos, Pumilio, and brain tumor proteins), which is recruited to the 3′ UTR via a Nanos responsive element (NRE) (4). Both translational repression mechanisms are required for the development of the *Drosophila* embryo by ensuring the correct asymmetric distribution of

Received 11 April 2012 Returned for modification 1 May 2012
Accepted 26 June 2012
Published ahead of print 2 July 2012
Address correspondence to Nahum Sonenberg, nahum.sonenberg@mcgill.ca.
M.M. and L.W.L. contributed equally to this article.
Supplemental material for this article may be found at http://mcb.asm.org/.

doi:10.1128/MCB.00455-12

Caudal and Hunchback proteins (4, 5). These studies demonstrate that d4EHP binding partners dictate its molecular and physiological functions. Recently, a homeobox protein, Prep1, has been shown to interact with murine 4EHP and inhibit the translation of *Hoxb4* mRNA (42). In this case, mice expressing a hypomorphic Prep1 allele manifest oocyte growth failure (42). These studies suggest that m4EHP, like d4EHP, may also function in embryonic development. Here, we identified GIGYF2 (Grb10-interacting GYF protein 2) and ZNF598 (zinc finger protein 598) as components of an m4EHP complex. We demonstrate that the m4EHP-GIGYF2 complex functions as a translational repressor and that it is essential for normal embryonic development in mice.

## MATERIALS AND METHODS

**Plasmids, antibodies, and siRNAs.** The HA-4EHP and Flag-HMK-4EHP plasmids (33) and the Myc-GIGYF2 and Myc-GIGYF1 plasmids (14) were described previously. The GIGYF2 mutant was generated by site-directed mutagenesis. Mouse monoclonal antibodies to hemagglutinin (HA) (MMS-101R), Myc (TAG003), β-actin (A5441), eIF4E (610270), and 4EHP (GTX103977) were purchased from Covance (Emeryville, CA), Bioshop Canada, Inc. (Burlington, Ontario, Canada), Sigma-Aldrich (St. Louis, MO), BD Transduction Laboratories (Mississauga, Ontario, Canada), and Gene-Tex, Inc. (Irvine, CA), respectively. Anti-GIGYF2 antibodies were described previously (14, 18). Horseradish peroxidase-conjugated anti-mouse and anti-rabbit secondary antibodies were from GE Healthcare. All small interfering RNAs (siRNAs) were from Dharmacon (Lafayette, CO). The sequences of siRNA are as follows: 4EHP siRNA, CUCACACCGACAGCAUCAAdTdT; and GIGYF2 siRNA, GGGAAGAG GAAGAGCGAAAdTdT.

**Cell culture, transfection, cell lysis, immunoprecipitation, and immunoblotting.** Plasmid transfections were carried out on HeLa S3 cells using Lipofectamine with Plus reagent (Invitrogen) according to the manufacturer's instructions. Cells were harvested 48 h after transfection in lysis buffer (50 mM Tris-HCl [pH 7.5], 150 mM NaCl, 1 mM EDTA, 1% NP-40, Roche complete protease inhibitor cocktail). For siRNA transfection, Lipofectamine 2000 (Invitrogen) was used. Cells were harvested 72 h after transfection in lysis buffer. Protein concentrations were estimated with the Bio-Rad protein assay. The procedure for immunoprecipitation and immunoblotting was described previously (28). For immunoprecipitation experiments, 1 mg of lysate was precleared using 50 μl of 50% protein G-Sepharose (GE Healthcare) for 1 h. Cleared lysates were incubated with 30 μl of 50% protein G-Sepharose preconjugated to the antibody of choice for 2 h at 4°C. Beads were washed with lysis buffer five times before reconstitution with SDS-PAGE sample buffer. Protein extracts were separated on SDS-PAGE and transferred to a nitrocellulose membrane. Immunoblotting was carried out using the indicated antibodies. Proteins were quantified on film using the ImageJ software (http://rsbweb.nih.gov/ij/index.html).

**Far-Western blot analysis.** The procedure for far-Western blot analysis was described previously (35). Flag-HMK-4EHP recombinant protein (5 μg) was radiolabeled with 5 μl of [γ-$^{32}$P]ATP (3,000 Ci/mmol), 3 μl of 10× heart muscle kinase (HMK) buffer (200 mM Tris-HCl [pH 7.5], 10 mM dithiothreitol [DTT], 1 M NaCl, 120 mM $MgCl_2$), and 10 U of HMK in a total volume of 30 μl at 4°C for 45 min. The radiolabeled protein probe was purified with a Pharmacia nick column (Sephadex G-50; GE Healthcare). After protein transfer, the membrane was prehybridized for 5 h at 4°C, with shaking, in prehybridization solution (20 mM HEPES-KOH [pH 7.7], 25 mM NaCl, 5 mM $MgCl_2$, 1 mM DTT, 0.1% NP-40, 5% skim milk), followed by far-Western buffer (25 mM HEPES-KOH [pH 7.7], 75 mM KCl, 2.5 mM $MgCl_2$, 0.1 mM EDTA, 1 mM DTT, 0.1% NP-40, 5% skim milk) containing 250,000 cpm/ml of the probe for 10 h at 4°C, with shaking. The membrane was washed three times with far-Western buffer for 15 min at 4°C followed by autoradiography. For mass spectrometry (MS) analysis, HeLa S3 cells stably expressing HA-4EHP were harvested in lysis buffer. The lysate was precleared with 100 μl protein G-Sepharose and immunoprecipitated in 70 μl of antibody cross-linked protein G-Sepharose. The immunoprecipitate was separated by keratin-free SDS-PAGE, and the gel was stained with Coomassie brilliant blue. The bands of interest were excised and analyzed by mass spectrometry as described previously (16).

**Cap-binding assay.** Cells were lysed by three freeze-thaw cycles in binding buffer (50 mM HEPES-KOH [pH 7.5], 150 mM KCl, 1 mM EDTA, 2 mM DTT, 0.2% Tween 20 and protease inhibitors). Protein concentration was measured by the Bio-Rad protein assay. One milligram of protein extract was incubated for 2 h at 4°C with 30 μl GDP or m$^7$GDP-agarose beads prepared as described previously (9). After incubation, the beads were washed five times with lysis buffer and eluted by boiling in the presence of 1× Laemmli buffer for 5 min.

**Affinity purification coupled to mass spectrometry.** 4EHP was amplified from clone MGC:4474 (mammalian gene collection; accession no. BC005874) and subcloned into the EcoRI and NotI sites of pcDNA3-Flag (11). *GIGYF2* was amplified by PCR from Myc-GIGYF2 (15) and subcloned into the AscI and NotI sites of pcDNA3-Flag. *ZNF598* was amplified from clone MGC:54362 (BC050477) and subcloned in the EcoRI and NotI sites of pcDNA3. All Flag-tagged constructs were stably expressed in pools of HEK293 cells, and expressed proteins were purified on anti-Flag M2-agarose beads, as described previously (3). For benzonase nuclease (EMD Biosciences) treatment, 500 U was added directly to the clarified lysate. Mass spectrometric analysis was conducted in a data-dependent mode (over a 2-h acetonitrile 2 to 40% gradient) on a Thermo LTQ mass spectrometer equipped with a Proxeon Nanosource and an Agilent capillary pump. RAW files were converted to MGF and searched (tolerance of 3 Da for the parent and 0.6 Da for the product ions; only +2 and +3 spectra were searched) using Mascot (Matrix Science, version 2.3) against the human and adenovirus complement of RefSeq (V45). Methionine oxidation and asparagine-glutamine oxidation were allowed as variable modifications, and up to one missed tryptic cleavage was allowed. All hits with ion scores of >35 were parsed into our relational database, ProHits (26), and analyzed in comparison to 2,000 other AP-MS analyses from HEK293 cells. (These databases include ~100 negative-control runs.) The following criterion was applied for filtering the list of potential interactors: interactions detected with a frequency in the database of ≥22% were deemed "frequent fliers" and omitted from further analysis. Only proteins detected with 5 or more unique peptides and 10 or more spectra were considered high-confidence interactors and reported here. The complete list of interactors that passed these filters is provided in Table S1 in the supplemental material. All of the raw mass spectrometry data for these experiments have been deposited in the Tranche repository (https://proteomecommons.org/tranche/), under hash WUDQwA9UFCvm/3Atj9VV5xJeAgZ6HGS7zQCR97QK3F+Zq1CDXf9zm2VtO4h9wY6CThXU9yyrda+n+oZcfG/2hgYwhsYAAAAAAAAE7Q==. To generate Fig. 5A, the spectral counts for each of the identified proteins were normalized, first to the length of each of the identified proteins and then to the ratio of bait spectra to bait length.

**Polysome analysis and [$^{35}$S]methionine metabolic labeling.** Polysome profile analysis was carried out as described previously (8). Briefly, mouse whole brain was homogenized in 450 μl of hypotonic buffer (5 mM Tris [pH 7.5], 2.5 mM $MgCl_2$, 1.5 mM KCl, protease inhibitors, 100 μg/ml cycloheximide, 2 mM DTT, 200 U/ml RNasin) with a Dounce glass homogenizer. Homogenates were vortexed briefly and lysed by the addition of detergents at the following final concentrations: 0.5% Triton X-100 and 0.5% sodium deoxycholate. Lysates were precleared by centrifugation at 21,000 × *g* for 5 min at 4°C, and the $A_{254}$ was measured to determine yield. Samples were loaded onto a sucrose gradient and were sedimented by velocity centrifugation at 36,000 × *g* for 2 h at 4°C using an SW40 rotor in a Beckman Coulter ultracentrifuge. Chasing solution (60% [wt/vol] sucrose) ran through the gradient, $A_{254}$ was measured, and fractions were collected. [$^{35}$S]methionine labeling was carried out as described previously (37). Briefly, the cells were seeded in 24-well plates. The

cells were grown for another 24 h, followed by an hour of methionine starvation in methionine-free media. The cells were incubated with medium containing [$^{35}$S]protein labeling mix for 45 min at 37°C. After the incubation, the cells were lysed with 1× Laemmli buffer. The lysates were boiled for 5 min, an aliquot was spotted on Whatman 1M paper, and the remaining lysates were visualized by SDS-PAGE. The paper was washed with trichloroacetic acid (TCA)–0.1% DL-methionine, 5% TCA, and ethanol. The paper was air dried and assayed for acid-insoluble radioactivity. [$^{35}$S]methionine labeling was carried out in triplicates and in three independent experiments.

**Generation of *4ehp* KO mice.** To generate *4ehp* knockout (KO) mice, a targeting construct contained a neomycin selection cassette flanked by two short flippase recognition target (FRT) sites was employed to generate a conditional allele (Fig. 6A). The targeting construct also contained two *loxP* sites between exons 3 and 4 and between exons 6 and 7 (Fig. 6A). E14 mouse embryonic stem (ES) cells were cultured under standard conditions on a feeder layer of G418-resistant primary embryonic fibroblasts. The targeting vector was linearized and electroporated into ES cells. The ES cells were cultured in the presence of G418 for selection. Positive clones were validated using PCR and were transfected with a plasmid encoding FLPase. Correctly targeted ES clones were used for microinjection. C57BL/6 female mice were used as blastocyst donors for microinjection. The highest percentage male chimeras were bred with C57BL/6J female mice to produce germ line-transmitted heterozygous mice. The F1 *4ehp*$^{+/flox}$ mice carrying the *Flox* allele were bred with cytomegalovirus promoter-induced *cre*-transgenic (CMV-*Cre*) mice to obtain mice with the *4ehp* null allele that had lost exons 4 to 6 but retained a single *loxP* site. Genotyping was carried out by PCR amplification of genomic DNA from tails using the set of primers shown in Fig. 6A. Amplification of wild-type (WT) genomic DNA yielded a single 800-bp PCR product, whereas *4ehp* null genomic DNA produced a 1-kb fragment as shown in Fig. 6B. All mouse experiments were carried out in accordance with the guidelines for animal use issued by the Committee of Animal Experiments, McGill University.

## RESULTS

**GIGYF proteins are m4EHP-binding partners.** In contrast to eIF4E, m4EHP does not interact with eIF4G and exhibits significantly lower affinity for 4E-BP1 (34, 47). This suggests that m4EHP likely associates with unique binding partners, in a manner similar to that described for d4EHP (4, 5). To identify m4EHP-interacting proteins, we first performed a far-Western analysis on HeLa S3 cell extracts using recombinant $^{32}$P-radiolabeled human 4EHP. Two prominent bands were visible on the autoradiograph, migrating approximately at 180 and 140 kDa (Fig. 1A). To identify these proteins, coimmunoprecipitation was performed using extracts from HeLa S3 cells stably expressing HA-4EHP. The coimmunoprecipitates were resolved by SDS-PAGE and visualized with Coomassie brilliant blue. Proteins migrating on the gel at a molecular mass similar to those identified by far-Western analysis were excised and analyzed by mass spectrometry (MS). GIGYF2 and GIGYF1, corresponding to bands 1 and 2, respectively (Fig. 1A), were identified as m4EHP-interacting proteins. To confirm that bands 1 and 2 were indeed GIGYF2 and GIGYF1, a far-Western analysis was performed on HeLa S3 cell extracts in which GIGYF2 and GIGYF1 were depleted with small interfering RNAs (siRNAs) (Fig. 1B, upper panel). The depletion resulted in a dramatic decrease in the intensity of bands 1 and 2 (Fig. 1B, lower panel), demonstrating that GIGYF2 and GIGYF1 bind to m4EHP *in vitro*.

As a result of the quantitative MS experiments (see below), which showed that m4EHP preferentially associates with GIGYF2 in HEK293 cells, we chose to further study the interaction of GIGYF2 and m4EHP. To verify that GIGYF2 protein associates

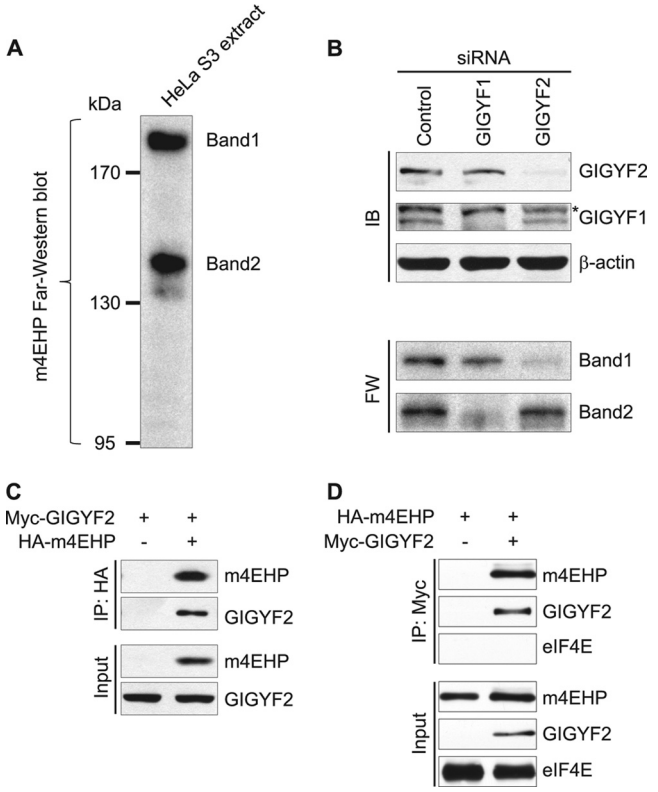


**FIG 1** Identification of GIGYF proteins as novel m4EHP-interacting partners. (A) Identification of 4EHP-binding proteins by far-Western analysis. Extracts from HeLa S3 cells were resolved by SDS-PAGE and transferred to nitrocellulose membrane, which was incubated with $^{32}$P-labeled recombinant 4EHP. Immunoprecipitates were separated by SDS-PAGE, the gel was stained with Coomassie brilliant blue, and the bands of interest were excised for MS analysis. MS identified GIGYF2 and GIGYF1 as candidates for bands 1 and 2, respectively. (B) GIGYF1 and GIGYF2 were depleted by siRNA in HeLa S3 cells. The levels of both proteins were specifically reduced, as demonstrated by immunoblotting (IB; upper panels). β-Actin served as a loading control. The asterisk denotes a nonspecific band. These lysates were subjected to far-Western analysis (FW; lower panels). (C) HeLa S3 cells were transfected with a Myc-GIGYF2 plasmid, with or without an HA-4EHP plasmid. Interactions were examined by coimmunoprecipitation (Co-IP) with anti-HA antibody, followed by immunoblotting (IB) with anti-Myc and anti-HA antibodies. (D) HeLa S3 cells were transfected with an HA-4EHP plasmid, with or without a Myc-GIGYF2 plasmid. Interactions were examined by Co-IP with anti-Myc antibody, followed by IB with anti-Myc, anti-HA, and anti-eIF4E antibodies. For panels C and D, inputs represent 10% of the total lysate used in the IP assay.

with m4EHP *in vivo*, immunoprecipitations of GIGYF2 and m4EHP from extracts of HeLa S3 cells expressing HA-4EHP and Myc-GIGYF2 were performed. Cell extracts were preincubated with RNase A to eliminate any indirect RNA-dependent interactions. Myc-GIGYF2 coimmunoprecipitated with HA-4EHP (Fig. 1C), and conversely, HA-4EHP coimmunoprecipitated with Myc-GIGYF2 (Fig. 1D). Notably, eIF4E failed to coimmunoprecipitate with Myc-GIGYF2 (Fig. 1D), indicating that GIGYF2 interacts specifically with m4EHP.

**GIGYF2 associates with m4EHP through a conserved binding motif.** In *Drosophila*, Bicoid interacts with d4EHP through a variant (YXYXXXXLΦ, where Φ is any hydrophobic amino acid) of the canonical eIF4E-binding motif (5). Mutation of this motif in Bicoid abolished its binding to d4EHP (5). We identified such a

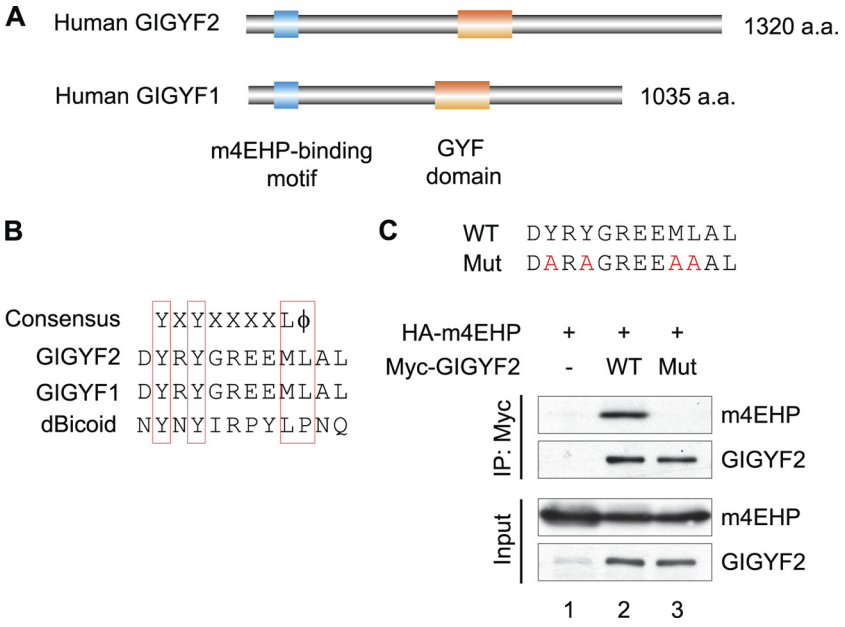


**FIG 2** Characterization of the interaction between m4EHP and GIGYF2. (A) Schematic representation of human GIGYF1 and GIGYF2 proteins. The m4EHP-binding motif and GYF domain are represented by blue and orange boxes, respectively. (B) Sequence alignment of the m4EHP consensus motif found in GIGYF2, GIGYF1, and the *Drosophila* 4EHP binding protein Bicoid (dBicoid). (C) HA-m4EHP and the wild-type/mutant Myc-GIGYF2 were ectopically expressed in HeLa S3 cells. Cell lysates were immunoprecipitated with anti-Myc antibody. Immunoblotting was performed with anti-Myc and anti-HA antibodies. Inputs represent 10% of the total lysate used in the IP assay.

motif at the N terminus of GIGYF1 and GIGYF2 (Fig. 2A and B) and generated a GIGYF2 construct in which the conserved amino acids were mutated (Fig. 2C). The mutant protein failed to associate with the coexpressed HA-m4EHP, as assessed by coimmunoprecipitation (Fig. 2C, lane 3). These results indicate that the GIGYF2 protein binds to m4EHP through a Bicoid-related d4EHP-binding motif.

**GIGFY2 binds to cap-bound m4EHP.** Since m4EHP binds the 5′ cap structure (34, 47), it was pertinent to determine whether GIGYF2 can bind to m4EHP in its cap-bound state. HeLa S3 cells were transfected with HA-4EHP and Myc-GIGYF2 constructs and cell extracts were incubated with agarose beads coupled to the cap analog, $m^7$GDP. GIGYF2 associated with m4EHP while it was bound to $m^7$GDP (Fig. 3A, lane 4). The m4EHP-GIGYF2 complex failed to form on GDP-coupled beads (lane 2), and GIGYF2 binding was dramatically diminished in the presence of $m^7$GDP (lane 3). Extracts from HeLa S3 cells expressing HA-4EHP and either the wild-type (WT) or m4EHP-binding site mutant of GIGYF2 (GIGYF2-Mut) were incubated with $m^7$GDP-coupled agarose beads. GIGYF2-WT, but not GIGYF2-Mut, bound to the $m^7$GDP beads, further demonstrating that GIGYF2 binding to m4EHP is dependent on the 4EHP-binding motif (Fig. 3B).

**m4EHP acts as a translational repressor and is stabilized by GIGYF2.** To investigate the biological significance of m4EHP interaction with GIGYF2, we depleted each protein from HeLa S3 cells using small interfering RNA (siRNA). 4EHP or GIGYF2 siRNA treatment resulted in an ~80% reduction and an ~90% reduction in protein expression, respectively (Fig. 4A). Strikingly, the depletion of m4EHP by siRNA led to a concomitant decrease in GIGYF2 protein (lane 2). Similarly, the depletion of GIGYF2 also decreased the abundance of m4EHP (lane 3), demonstrating that the stabilities of m4EHP and GIGYF2 proteins are coregulated.

Next, we examined the effect of m4EHP and GIGYF2 depletion on general protein synthesis, by using [$^{35}$S]methionine metabolic labeling. m4EHP silencing engendered an ~30% increase in [$^{35}$S]methionine incorporation compared to control siRNA-transfected cells (Fig. 4B and C). Similarly, the depletion of GIGYF2 led to an ~30% increase in [$^{35}$S]methionine incorpora-

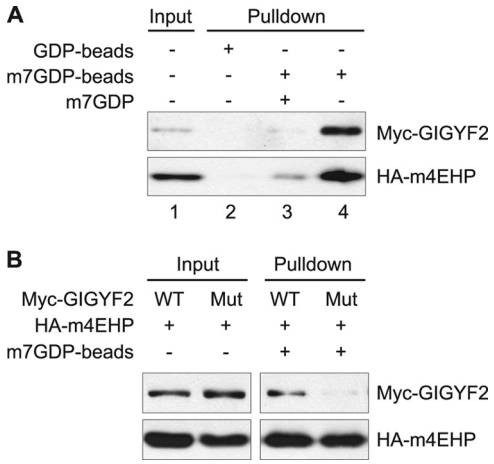


**FIG 3** GIGYF2 associates with cap-bound m4EHP. (A) HeLa S3 cells were cotransfected with Myc-GIGYF2 and HA-m4EHP. Lysates were incubated with either GDP- or $m^7$GDP-coupled agarose beads (lanes 2 and 4). Cap-bound proteins were eluted from the beads and resolved by SDS-PAGE. Free $m^7$GDP was used to confirm the specific binding of HA-m4EHP and Myc-GIGYF2 to the $m^7$GDP cap (lane 3). (B) HeLa S3 cells were cotransfected with HA-m4EHP and either the wild-type (WT) or m4EHP binding mutant (Mut) Myc-GIGYF2. Cell lysates were incubated with $m^7$GDP-coupled agarose beads. Immunoblotting was performed with anti-Myc and anti-HA antibodies. Inputs represent 5% of the total lysate used in the pulldown assay.

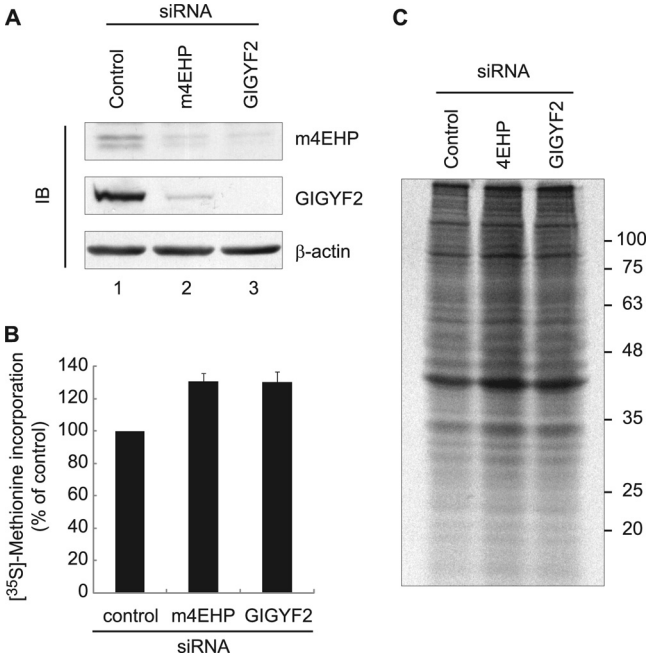


**FIG 4** The rate of protein synthesis is increased in m4EHP- and GIGYF2-depleted cells. (A) Immunoblotting of 4EHP and GIGYF2 in HeLa cells transfected with control, m4EHP, or GIGYF2 siRNAs. β-Actin was used as a loading control. The doublet observed on the topmost Western blot corresponds to m4EHP (33). (B) Effects of m4EHP or GIGYF2 silencing on protein synthesis. Protein synthesis was measured by [$^{35}$S]methionine incorporation normalized to the total amount of protein. The value of the control cells was adjusted to 100%. [$^{35}$S]methionine labeling was carried out in triplicates and in three independent experiments ($n = 3$). All values represent means ± standard deviations (SD). (C) Control or siRNA-treated HeLa cells were pulse-labeled with [$^{35}$S]methionine. Newly synthesized proteins were visualized by SDS-PAGE and autoradiography. Equal amounts of sample were loaded. Numbers to the right indicate molecular masses (kDa).

tion (Fig. 4B and C). Due to the coregulation of m4EHP and GIGYF2 protein expression, it is not possible to dissociate the activities of m4EHP and GIGYF2 using this assay. These observations indicate that the m4EHP and/or GIGYF2 proteins repress translation.

**m4EHP, GIGYF2, and zinc finger 598 form a complex.** *Drosophila* Bicoid contains a d4EHP binding motif and an RNA recognition motif (RRM) that recognizes the Bicoid binding region in the 3′ UTR of *caudal* mRNA (5). Thus, Bicoid tethers the 5′ and 3′ ends of the mRNA and impairs *caudal* mRNA translation. Sequence analysis of GIGYF2 identified a glycine-tyrosine-phenylalanine (GYF)-proline-rich sequence binding domain, but no RNA binding motif (Fig. 2A). Assuming that the translation repression mechanism would be similar to that observed in *Drosophila* (16), m4EHP-GIGYF2 would require an RNA-binding protein to bind to the mRNA 3′ UTR. To identify additional binding partners that could potentially bind RNA, we performed affinity purification coupled with mass spectrometry (AP-MS), using stably expressed Flag-tagged m4EHP. To ensure that the interactions detected with m4EHP were mediated via protein-protein interactions, rather than via RNA tethering, the nuclease benzonase was used (another sample was analyzed without benzonase treatment [see Table S1 in the supplemental material]) (16). After background subtraction, high-confidence interacting partners for m4EHP were identified (Fig. 5A). Corroborating our far-Western/MS analysis, a large number of peptides and extensive coverage were found for GIGYF2 and, to a lesser extent, GIGYF1. Notably, next to GIGYF2, the zinc finger protein 598 (ZNF598) was identified by the highest number of spectra, in agreement with an earlier report identifying ZNF598 as a GIGYF2-associated protein in mass spectrometric analysis (1). An interaction of m4EHP with 4E-T was also observed by AP-MS (Fig. 5A), which could be recapitulated in a reciprocal AP-MS experiment (data not shown). However, we did not further characterize this interaction.

To investigate how m4EHP complexes are assembled, we stably expressed Flag-tagged GIGYF2 and ZNF598 separately in HEK293 cells and performed AP-MS analysis. Flag-GIGYF2 associated with m4EHP and ZNF598, but GIGYF1 was not detected in this screen (Fig. 5A; see Table S1 in the supplemental material). Similarly, Flag-ZNF598 was associated with GIGYF2 and m4EHP, but not with GIGYF1. These results suggest a preference for m4EHP, GIGYF2, and ZNF598 complex formation. The association of m4EHP, GIGYF2, and ZNF598 was validated by performing triple-transfection experiments followed by immunoprecipitation/Western blotting of HA-4EHP, Flag-ZNF598, and Myc-GIGYF2 or Myc-GIGYF2-mut (Fig. 5B). FLAG-ZNF598 coimmunoprecipitated with WT and mutant Myc-GIGYF2. However, FLAG-ZNF598 failed to coimmunoprecipitate with HA-m4EHP when cotransfected with Myc-GIGYF2-mut (Fig. 5B). This experiment shows that ZNF598 associates with m4EHP through binding to GIGYF2.

**Disruption of the *4ehp* gene in mice.** Our previous studies documented the function of d4EHP in *Drosophila* development (4, 5). We hypothesized that mammalian 4EHP could have a similar role and therefore generated mice with a *4ehp* gene disruption to study its role in development. The targeting strategy used to disrupt the *4ehp* gene located on mouse chromosome 1D1 is illustrated in Fig. 6A. The resulting knockout (KO) progeny lacked exons 4, 5, and 6 of m4EHP, which encode the main portion of the protein (amino acids 91 to 222 out of 245), including the cap-binding site (33, 34). Successful generation of the KO mice was confirmed by PCR analysis (Fig. 6B). Immunoblotting of extracts from mouse embryonic fibroblasts (MEFs) confirmed the absence of m4EHP (Fig. 6C).

Next, we compared the tissue expression patterns of the m4EHP and GIGYF2 proteins in mouse embryos. m4EHP and GIGYF2 proteins are widely expressed (18, 33) but are enriched in the brain and lungs at embryonic day 18.5 (E18.5) (Fig. 7A). Consistent with the findings from siRNA-treated cells (Fig. 4A), there was a decrease of GIGYF2 protein in *4ehp* KO MEFs (Fig. 6C) and in the brain and lungs (Fig. 7A). Notably, a loss of m4EHP had no effect on the expression of eIF4E (Fig. 7A). Next, we compared the polysome profiles from WT and *4ehp* KO tissue. Depletion of the m4EHP and GIGYF2 proteins in the brain caused a shift toward heavier polysomes, with a concomitant decrease in the abundance of 80S ribosomes (Fig. 7B). Since the absence of m4EHP causes an increase in translation (Fig. 4B), these findings demonstrate that m4EHP plays a physiological role as a translational repressor *in vivo*.

**Phenotypic analysis of the *4ehp* knockout mice.** Heterozygous mice are viable and fertile and developed normally. However, intercrossing of *4ehp* heterozygous mice did not yield any viable *4ehp* KO mice (Fig. 8A). All *4ehp* KO newborns were dead at postnatal day 0 (P0) (Fig. 8A, B, And C). Analysis of the *4ehp* KO

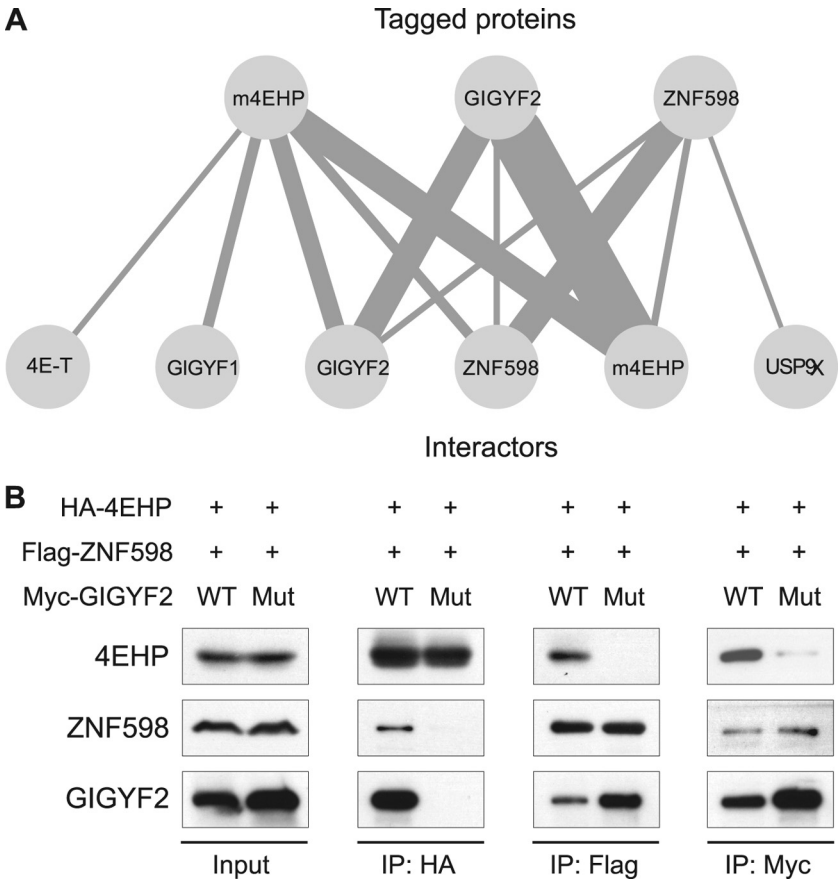


**FIG 5** The mammalian m4EHP interaction network. (A) Cytoscape (38) figure displaying the high-confidence interaction partners by AP-MS. The top row represents bait proteins that were tagged and purified. The bottom row shows the protein hits identified by MS. The thickness of the connectors reflects the total number of spectra acquired for each bottom protein. (B) HEK293T cells were triply transfected with HA-4EHP, Flag-ZNF598, and Myc-GIGYF2-WT or Myc-GIGYF2-Mut expression vectors. Interactions were examined by coimmunoprecipitation (Co-IP) with anti-HA, anti-FLAG, and anti-Myc antibodies followed by immunoblotting (IB) with anti-HA, anti-FLAG, and anti-Myc antibodies. Input represents 10% of the total lysate used in the IP assay.

embryos, just before birth, showed a normal Mendelian ratio of genotypes up to 18.5 days postconception (E18.5), indicating that lethality occurred perinatally (Fig. 8A). The *4ehp* KO embryos differed from their littermate controls in several phenotypes. First, the *4ehp* KO embryos were cyanotic at birth. Second, the body weight of *4ehp* KO embryos was significantly lower than those of wild-type or *4ehp* heterozygous embryos (Fig. 8D). Finally, anatomical analysis of *4ehp* KO mice revealed smaller brains and unexpanded lungs (see Fig. S1 in the supplemental material). All *4ehp* KO embryos died within a few hours of birth, underscoring the importance of m4EHP during embryonic development.

## DISCUSSION

eIF4E homologous protein (4EHP) was first discovered in humans and subsequently studied in other species, including *Arabidopsis thaliana* (36), *Caenorhabditis elegans* (6, 23), and *Drosophila melanogaster* (4, 5). 4EHP homologs (referred to as the eIF4E-2 class) exist in many metazoan, plant, and fungal species (22). 4EHP performs essential functions in normal embryonic development in *C. elegans* (6, 23) and *Drosophila* (4, 5). In this study, we identified GIGYF2 as a novel mammalian 4EHP binding partner and characterized the function of the m4EHP-GIGYF2 complex in translation regulation and development.

GIGYF2 was identified as an interacting protein of Grb10, an adapter protein of insulin and insulin-like growth factor I (IGF-I) receptors, and thus was proposed to have a role in regulating receptor signaling (15, 18). GIGYF2 is a 150-kDa protein containing a GYF domain that specifically binds to proline-rich sequences (25). Our study shows that GIGYF2 interacts directly with free and cap-bound 4EHP through a site highly similar to the Bicoid d4EHP-binding motif (Fig. 2 and 3). The 4EHP motif is also similar to the canonical eIF4E binding motif found in eIF4G, 4E-BPs, and 4E-T (45). Since eIF4E-interacting proteins bind the dorsal surface of eIF4E (27), which is distal to the 5′ cap-binding site, it is likely that GIGYF2 interaction occurs at the dorsal surface of 4EHP in a similar manner. In a previous study, 4EHP was found to be 5 to 10 times less abundant than eIF4E (33). Coupled with the results showing that 4EHP has ~100- to 200-fold lower affinity for the 5′ cap than eIF4E (34, 47), it is unlikely that 4EHP alone can directly compete with eIF4E for the cap structure. Hence 4EHP binding partners, such as GIGYF2, are likely to increase 4EHP binding affinity for the 5′ cap via RNA tethering, in a manner similar to eIF4G enhancement of eIF4E binding to the cap (44, 46). The interaction between m4EHP and GIGYF2 is important not only for function but also for their mutual stability, inasmuch as the depletion of 4EHP by siRNA in human cell lines or disrup-

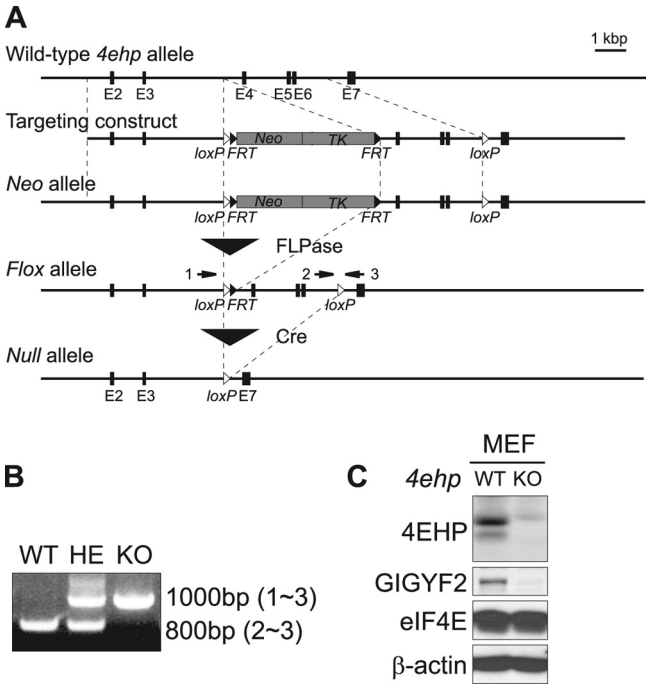


**FIG 6** Disruption of the *4ehp* gene in mice. (A) Schematic representation of the targeting construct used for the generation of *4ehp* knockout mice. *FRT* and *loxP* sequences are indicated by black and white triangles, respectively. Negative (HSV-*TK*) and positive (*PGK-neo*) selection markers are indicated by gray boxes (*TK*, thymidine kinase; *Neo*, neomycin). Numbered black boxes represent exons in the *4ehp* gene. The *4ehp neo* allele was produced by homologous recombination. FLPase was used to generate the *4ehp flox* allele. *4ehp* null allele mice were produced by mating *flox* allele males with CMV-Cre females. (B) PCR genotyping of genomic DNA from mice with the *4ehp* wild-type (WT), heterozygous (HE), and knockout (KO) genotypes. Arrows (numbered 1 to 3) in panel A denote annealing positions of oligonucleotides used for genotyping. (C) Immunoblotting of m4EHP, GIGYF2, and eIF4E proteins in *4ehp* WT and KO MEFs. β-Actin was used as a loading control.

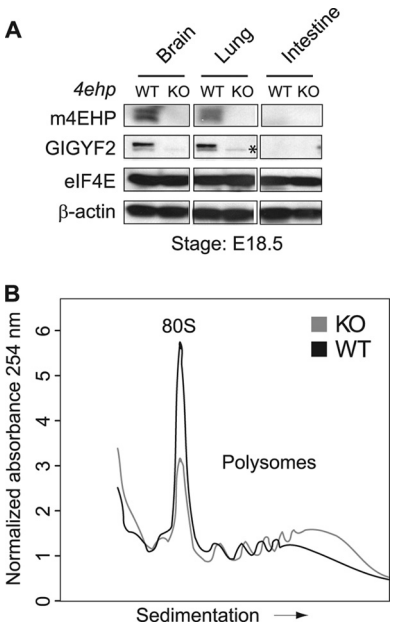


**FIG 7** Tissue distribution of m4EHP-GIGYF2 proteins and polysome profile of wild-type and *4ehp* knockout mice. (A) Immunoblotting of m4EHP, GIGYF2, and eIF4E proteins in *4ehp* WT and KO tissues isolated from mice at E18.5. β-Actin was used as a loading control. An asterisk denotes a nonspecific band. (B) Polysome profiles of WT and *4ehp* KO whole-brain lysates. Brain lysates were sedimented on 10% to 50% sucrose gradients. $A_{254}$ was continuously recorded. Polysome profiles were normalized with the area under the curve. 80S denotes the monosome peak.

tion of the *4ehp* gene in mice resulted in less GIGYF2 protein (Fig. 4A and 6C). Similarly, GIGYF2 depletion also leads to a decrease in 4EHP, indicating that the intracellular levels of both proteins are mutually coregulated (Fig. 4A).

Given that 4EHP is essential for normal embryonic development in *Drosophila* (5) and *C. elegans* (6), we hypothesized that m4EHP could play a similar role. To investigate the physiological function of m4EHP, we generated a knockout mouse (Fig. 6). The *4ehp* KO mice displayed perinatal mortality in the hours following natural birth (Fig. 8). Notably, a comparable phenotype is also observed in the GIGYF2 KO mouse, where newborn pups die within the first 2 postnatal days (15), consistent with the fact that m4EHP and GIGYF2 are mutually coregulated. Perinatal lethal phenotypes can occur due to a variety of physiological defects, including stress during birthing itself or defects related to respiration, suckling, and homeostasis (41). Since *4ehp* KO embryos were cyanotic after birth, this suggests a defect in respiration, which can be due to problems with the lungs, central nervous system, muscles involved in breathing, or malfunctions of the face and respiratory tract (41). Thus, it is difficult to ascertain the exact cause of death. However, the tissue distribution of m4EHP and GIGYF2 proteins implies their importance in neurogenesis and lung development (Fig. 7A). Additional studies will be required to reveal the exact physiological role of the m4EHP-GIGYF2 complex. Nonetheless, these results indicate that m4EHP and GIGYF2 work in concert to control essential developmental processes.

The *4ehp* knockout mouse was generated by targeting the gene located on chromosome 1D1. It is intriguing that *Gigyf2* is also located in the vicinity of *4ehp* on chromosome 1 in mice. This is also the case in humans, where the *4EHP* (*EIF4E2*) and *GIGYF2* genes are mapped to the 2q37.1 region. Genes that are located on the same locus and are part of the same biochemical pathway are commonly conserved throughout mammalian species (30). For instance, in humans, a large proportion of the cardiac transcriptome is linearly arranged in small groups of adjacent genes and each group tends to be regulated by the same transcription factor (43). The relationship between genomic organization, regulation, and gene function in higher eukaryotes remains to be precisely defined. However, there is much evidence to support the idea of a link between chromosomal gene order, transcriptional regulation, gene expression patterns, and biochemical function (19). As m4EHP and GIGYF2 protein stabilities are coregulated, it is likely that their genes, which are organized in a linear arrangement, are expressed in concert for coordinated control.

Our results (Fig. 4B and C and 7B) demonstrate that m4EHP and GIGYF2 act together as translational repressors *in vivo*. m4EHP depletion resulted in a 30% increase in [$^{35}$S]methionine incorporation into proteins (Fig. 4B and C) and an increase in polysomes (Fig. 7B). These results suggest that m4EHP regulates either a substantial number of mRNAs or a small number of mRNAs that represent a significant part of the total translation profile. d4EHP inhibits the translation of certain mRNAs (*caudal* and *hunchback*) by simultaneously binding the 5′ cap- and RNA-

A

| Stage | Number | | | Total |
|---|---|---|---|---|
| | WT | HE | KO | |
| Postnatal day 0 | 22 | 42 | 7[a] | 71 |
| Embryonic day 18.5 | 6 | 19 | 7 | 32 |

[a] All mice were dead

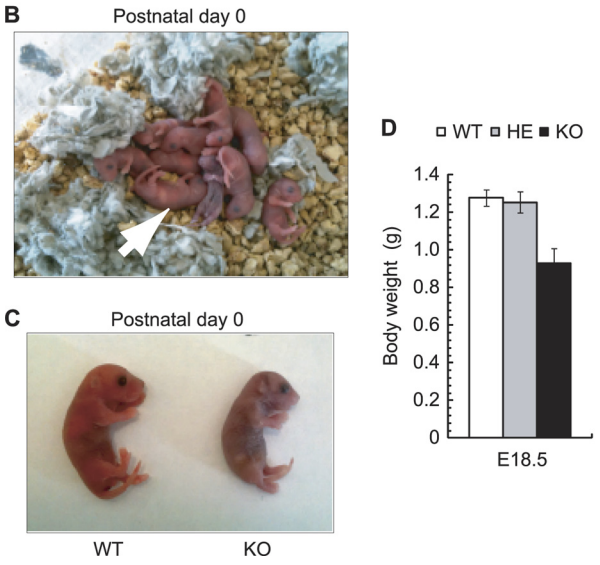


**FIG 8** Perinatal lethality in *4ehp* knockout mice. (A) Summary of *4ehp* heterozygous intercrosses. Genotyping of embryos and pups at indicated stages was performed by PCR. (B and C) Gross appearance of *4ehp* WT and KO pups at postnatal day 0. The arrow indicates a *4ehp* KO pup. (D) Body weight of *4ehp* WT, heterozygous (HE), and KO pups at E18.5. All values represent means ± SD. $n = 5$ for each genotype.

binding proteins (Bicoid) or protein complexes (NRE) bound to the mRNA 3′ UTR (4, 5). Accordingly, we propose that the m4EHP-GIGYF2 complex proteins work together to repress the translation of a subset of mRNAs through RNA-binding proteins which bind the 3′ UTR of mRNA. The AP-MS experiments demonstrate that ZNF598 preferentially associates with the 4EHP-GIGYF2 complex (as opposed to m4EHP-GIGYF1) (Fig. 5; see Table S1 in the supplemental material). Zinc finger domains are known to play multiple cellular roles from protein-protein interaction to nucleotide (both DNA and RNA) binding (24). In addition, stable isotope labeling by amino acids in cell culture (SILAC)/MS experiments showed that GIGYF2 associates with a variety of RNA-binding proteins, such as HuR, FXR1, and G3BP1 (1). Therefore, it is plausible that these RNA-binding proteins play a key role in the recruitment of the m4EHP-GIGYF2 complex to the target mRNA.

## ACKNOWLEDGMENTS

We thank D. Labbe, M. Livingstone, and A. Yanagiya for stimulating discussions and C. Lister, I. Harvey, P. Kirk, A. Sylvestre, and S. Perreault for technical assistance.

This work was supported by grants from the Canadian Institute of Health Research (CIHR) and the Canadian Cancer Society (CCS) to N. Sonenberg and from the CIHR (MOP-84314) to A.-C.G., the Uehara Memorial Foundation and the JSPS Excellent Young Researcher Overseas Visit Program to M.M., the CCS to M.F., the Cole Foundation to N. Siddiqui, the Swedish Research Council, the Swedish Cancer Foundation, the Cancer Society in Stockholm, the Jeansson Foundation, and the Åke Wiberg Foundation to O.L., and CIHR and the Terry Fox Research Institute to I.T. A.-C.G. is the Lea Reichmann Chair in Cancer Proteomics and the Canada Research Chair in Functional Proteomics.

## REFERENCES

1. **Ash MR, et al.** 2010. Conserved beta-hairpin recognition by the GYF domains of Smy2 and GIGYF2 in mRNA surveillance and vesicular transport complexes. Structure **18**:944–954.
2. **Chekulaeva M, Hentze MW, Ephrussi A.** 2006. Bruno acts as a dual repressor of oskar translation, promoting mRNA oligomerization and formation of silencing particles. Cell **124**:521–533.
3. **Chen GI, et al.** 2008. PP4R4/KIAA1622 forms a novel stable cytosolic complex with phosphoprotein phosphatase 4. J. Biol. Chem. **283**:29273–29284.
4. **Cho PF, et al.** 2006. Cap-dependent translational inhibition establishes two opposing morphogen gradients in Drosophila embryos. Curr. Biol. **16**:2035–2041.
5. **Cho PF, et al.** 2005. A new paradigm for translational control: inhibition via 5′-3′ mRNA tethering by Bicoid and the eIF4E cognate 4EHP. Cell **121**:411–423.
6. **Dinkova TD, Keiper BD, Korneeva NL, Aamodt EJ, Rhoads RE.** 2005. Translation of a small subset of *Caenorhabditis elegans* mRNAs is dependent on a specific eukaryotic translation initiation factor 4E isoform. Mol. Cell. Biol. **25**:100–113.
7. **Dostie J, Ferraiuolo M, Pause A, Adam SA, Sonenberg N.** 2000. A novel shuttling protein, 4E-T, mediates the nuclear import of the mRNA 5′ cap-binding protein, eIF4E. EMBO J. **19**:3142–3156.
8. **Dowling RJ, et al.** 2010. mTORC1-mediated cell proliferation, but not cell growth, controlled by the 4E-BPs. Science **328**:1172–1176.
9. **Edery I, Altmann M, Sonenberg N.** 1988. High-level synthesis in Escherichia coli of functional cap-binding eukaryotic initiation factor eIF-4E and affinity purification using a simplified cap-analog resin. Gene **74**:517–525.
10. **Ferraiuolo MA, et al.** 2005. A role for the eIF4E-binding protein 4E-T in P-body formation and mRNA decay. J. Cell Biol. **170**:913–924.
11. **Gingras AC, et al.** 2005. A novel, evolutionarily conserved protein phosphatase complex involved in cisplatin sensitivity. Mol. Cell. Proteomics **4**:1725–1740.
12. **Gingras AC, et al.** 1999. Regulation of 4E-BP1 phosphorylation: a novel two-step mechanism. Genes Dev. **13**:1422–1437.
13. **Gingras AC, Raught B, Sonenberg N.** 1999. eIF4 initiation factors: effectors of mRNA recruitment to ribosomes and regulators of translation. Annu. Rev. Biochem. **68**:913–963.
14. **Giovannone B, et al.** 2003. Two novel proteins that are linked to insulin-like growth factor (IGF-I) receptors by the Grb10 adapter and modulate IGF-I signaling. J. Biol. Chem. **278**:31564–31573.
15. **Giovannone B, et al.** 2009. GIGYF2 gene disruption in mice results in neurodegeneration and altered insulin-like growth factor signaling. Hum. Mol. Genet. **18**:4629–4639.
16. **Goudreault M, et al.** 2009. A PP2A phosphatase high density interaction network identifies a novel striatin-interacting phosphatase and kinase complex linked to the cerebral cavernous malformation 3 (CCM3) protein. Mol. Cell. Proteomics **8**:157–171.
17. **Haghighat A, Mader S, Pause A, Sonenberg N.** 1995. Repression of cap-dependent translation by 4E-binding protein 1: competition with p220 for binding to eukaryotic initiation factor-4E. EMBO J. **14**:5701–5709.
18. **Higashi S, et al.** 2010. GIGYF2 is present in endosomal compartments in the mammalian brains and enhances IGF-1-induced ERK1/2 activation. J. Neurochem. **115**:423–437.
19. **Hurst LD, Pal C, Lercher MJ.** 2004. The evolutionary dynamics of eukaryotic gene order. Nat. Rev. Genet. **5**:299–310.
20. **Jackson RJ, Hellen CU, Pestova TV.** 2010. The mechanism of eukaryotic translation initiation and principles of its regulation. Nat. Rev. Mol. Cell Biol. **11**:113–127.
21. **Joshi B, Cameron A, Jagus R.** 2004. Characterization of mammalian eIF4E-family members. Eur. J. Biochem. **271**:2189–2203.
22. **Joshi B, Lee K, Maeder DL, Jagus R.** 2005. Phylogenetic analysis of eIF4E-family members. BMC Evol. Biol. **5**:48. doi:10.1186/1471-2148-5-48.

23. **Keiper BD, et al.** 2000. Functional characterization of five eIF4E isoforms in Caenorhabditis elegans. J. Biol. Chem. **275**:10590–10596.
24. **Klug A.** 2010. The discovery of zinc fingers and their applications in gene regulation and genome manipulation. Annu. Rev. Biochem. **79**:213–231.
25. **Kofler MM, Freund C.** 2006.The GYF domain. FEBS J. **273**:245–256.
26. **Liu G, et al.** 2010. ProHits: integrated software for mass spectrometry-based interaction proteomics. Nat. Biotechnol. **28**:1015–1017.
27. **Marcotrigiano J, Gingras AC, Sonenberg N, Burley SK.** 1999. Cap-dependent translation initiation in eukaryotes is regulated by a molecular mimic of eIF4G. Mol. Cell **3**:707–716.
28. **Morita M, et al.** 2011. Obesity resistance and increased hepatic expression of catabolism-related mRNAs in Cnot3(+/−) mice. EMBO J. **30**:4678–4691.
29. **Nakamura A, Sato K, Hanyu-Nakamura K.** 2004. Drosophila cup is an eIF4E binding protein that associates with Bruno and regulates oskar mRNA translation in oogenesis. Dev. Cell **6**:69–78.
30. **O'Brien SJ, et al.** 1999. The promise of comparative genomics in mammals. Science **286**:458–462, 479–481.
31. **Pause A, et al.** 1994. Insulin-dependent stimulation of protein synthesis by phosphorylation of a regulator of 5′-cap function. Nature **371**:762–767.
32. **Richter JD, Sonenberg N.** 2005. Regulation of cap-dependent translation by eIF4E inhibitory proteins. Nature **433**:477–480.
33. **Rom E, et al.** 1998. Cloning and characterization of 4EHP, a novel mammalian eIF4E-related cap-binding protein. J. Biol. Chem. **273**:13104–13109.
34. **Rosettani P, Knapp S, Vismara MG, Rusconi L, Cameron AD.** 2007. Structures of the human eIF4E homologous protein, h4EHP, in its m7GTP-bound and unliganded forms. J. Mol. Biol. **368**:691–705.
35. **Roy G, et al.** 2002. Paip1 interacts with poly(A) binding protein through two independent binding motifs. Mol. Cell. Biol. **22**:3769–3782.
36. **Ruud KA, Kuhlow C, Goss DJ, Browning KS.** 1998. Identification and characterization of a novel cap-binding protein from Arabidopsis thaliana. J. Biol. Chem. **273**:10325–10330.
37. **Shahbazian D, et al.** 2010. Control of cell survival and proliferation by mammalian eukaryotic initiation factor 4B. Mol. Cell. Biol. **30**:1478–1485.
38. **Shannon P, et al.** 2003. Cytoscape: a software environment for integrated models of biomolecular interaction networks. Genome Res. **13**:2498–2504.
39. **Sonenberg N, Hinnebusch AG.** 2009. Regulation of translation initiation in eukaryotes: mechanisms and biological targets. Cell **136**:731–745.
40. **Stebbins-Boaz B, Cao Q, de Moor CH, Mendez R, Richter JD.** 1999. Maskin is a CPEB-associated factor that transiently interacts with elF-4E. Mol. Cell **4**:1017–1027.
41. **Turgeon B, Meloche S.** 2009. Interpreting neonatal lethal phenotypes in mouse mutants: insights into gene function and human diseases. Physiol. Rev. **89**:1–26.
42. **Villaescusa JC, et al.** 2009. Cytoplasmic Prep1 interacts with 4EHP inhibiting Hoxb4 translation. PLoS One **4**:e5213. doi:10.1371/journal.pone.0005213.
43. **Vogel JH, von Heydebreck A, Purmann A, Sperling S.** 2005. Chromosomal clustering of a human transcriptome reveals regulatory background. BMC Bioinformatics **6**:230. doi:10.1186/1471-2105-6-230.
44. **von der Haar T, Ball PD, McCarthy JE.** 2000. Stabilization of eukaryotic initiation factor 4E binding to the mRNA 5′-cap by domains of eIF4G. J. Biol. Chem. **275**:30551–30555.
45. **von der Haar T, Gross JD, Wagner G, McCarthy JE.** 2004. The mRNA cap-binding protein eIF4E in post-transcriptional gene expression. Nat. Struct. Mol. Biol. **11**:503–511.
46. **Yanagiya A, et al.** 2009. Requirement of RNA binding of mammalian eukaryotic translation initiation factor 4GI (eIF4GI) for efficient interaction of eIF4E with the mRNA cap. Mol. Cell. Biol. **29**:1661–1669.
47. **Zuberek J, et al.** 2007. Weak binding affinity of human 4EHP for mRNA cap analogs. RNA **13**:691–697.